1517

SUB OPTICS LETTERS 22/9/97

All-Optical 'AND' Gate Based on Coupled Gap Soliton Formation in a Fibre Bragg Grating

D.Taverner, N.G.R. Broderick, D.J. Richardson, M. Ibsen, R.I. Laming.

Optoelectronics Research Centre, Southampton University,

Southampton, SO17 1BJ, UK.

Abstract: We experimentally demonstrate an all-optical 'AND' gate based on coupled gap soliton formation in an unchirped fibre Bragg grating. A switching contrast of better than 17dB is obtained with an incident pulse peak power of 2.5kW.

All-Optical 'AND' Gate Based on Coupled Gap Soliton Formation in a Fibre Bragg Grating

D.Taverner, N.G.R. Broderick, D.J. Richardson, M. Ibsen, R.I. Laming.

Optoelectronics Research Centre, Southampton University,

Southampton, SO17 1BJ, UK.

The formation and properties of gap solitons in nonlinear periodic media have been well studied and documented on a theoretical basis [1,2,3]. Much like a conventional soliton propagating in an optical fibre, the gap soliton is maintained through a balance between group-velocity dispersion and nonlinear self phase modulation with the dispersion in this case provided by the photonic band gap of a Bragg grating. The strong dispersion associated with these structures means that a correspondingly strong nonlinear interaction is needed for gap soliton formation which has hindered their experimental observation to date. However, recent advances in photorefractive fibre Bragg grating (FBG) fabrication have brought the nonlinear thresholds for gap soliton formation within attainable levels. Although the nonlinear index of silica glass is relatively small, the long, >1m interaction lengths achievable in FBGS make them a most promising system for the study of gap soliton effects. Indeed using an FBG we have recently demonstrated for the first time the generation and propagation of gap solitons at frequencies lying within the bandgap of a Bragg grating [4].

Amongst the proposed applications for these nonlinear pulses is their use in all-optical logic gates. A specific proposal for an all-optical 'AND' gate was put forward by S. Lee and S.T. Ho [5]. The operational principle of their gate is based on the formation and transmission of coupled gap solitons through Bragg grating resulting from the combined effects of dispersion and both self-phase and cross-phase modulation induced by two orthogonally polarised beams with frequencies lying within the bandgap of the grating. Individually however, each input (polarisation component) is below the threshold for gap soliton formation and therefore is highly reflected. We note that cw operation of such a system has been described by Samir, et al [6]. In work presented here we experimentally demonstrate for the first time the operation of such a gap soliton logic gate.

The experimental set-up is shown in Figure 1 and apart from the beam splitting optics described below was identical to that used in reference [4]. The linearly polarised incident beam is split with a $\lambda/2$ waveplate (WP1) and polarisation beamsplitter (PBS) combination, providing two inputs, A and B, to the FBG. After following equal length paths these beams are recombined at a second PBS and launched into the FBG. The intensity of beam A incident on the grating was controlled by rotation of the $\lambda/2$ waveplate (WP2) preceding this second PBS. Finally, a third $\lambda/2$ waveplate (WP3) allowed rotation of the orthogonally polarised incident beams relative to the FBG birefringence axes. The transmitted and incident signals were detected with a single-mode fibre coupled PIN photodiode and sampling oscilloscope. Our temporal resolution was ~50ps. The fibre grating was written into a germanosilicate fibre with a mode-area of 30μm^2 (N.A.=0.25, λ_C=1250nm) using a moving fibre/phase-mask scanning beam technique similar to that reported in [7]. The grating was 8cm long, unchirped, with a 0-π sinusoidal apodisation profile along its length. Figure 2 shows reflection time-delay and amplitude response measurements made on the two birefringence axes of the FBG. The observed reflectivity peak wavelength separation between the two axes was 0.006nm and corresponds to a fibre birefringence of 4×10^{-6}. The grating had 98% reflectivity at its peak wavelength of 1536nm and was measured to have a 3dB bandwidth of 4.1GHz with strongly suppressed sidelobes (see figure 2), as expected from the apodisation profile used. The theoretical bandwidth of a perfect grating with such parameters was calculated to be approximately 3.9GHz, demonstrating the high quality of the fabrication process over such lengths. The grating was mounted in a glass capillary and angle polished front and back to remove unwanted reflections from these surfaces. The high power pulses were obtained from a large mode area, erbium doped fibre amplifier chain seeded with 10ns pulses from a directly-modulated, wavelength-tunable, semiconductor DFB laser [8]. The source was capable of producing nanosecond pulses with energies >100μJ and peak powers >100kW at kHz repetition rates with a linear output polarization state. For the purposes of this experiment the source was operated at 4kHz repetition rate giving 25μJ pulses with ≈2ns duration (see insert Figure 1). Note that the pulse is highly asymmetric due to amplifier saturation effects and has a sharp ~30ps feature on the leading edge due to chirp on the diode seed pulse. This feature becomes more prominent when examining the pulse transmission through the FBG with the pulse spectrum tuned to lie within the band-gap (see Fig 3, traces A and B). The chirped spike lies outside the band gap and is transmitted whereas the main body of the pulse is reflected. Although aesthetically undesirable this feature actually proved a valuable calibration aid, giving a direct measure in the transmitted pulse time domain of the input pulse power. The pulse spectrum at the FBG input was measured to have a 3dB spectral bandwidth of 1.2GHz, considerably less than the FBG bandwidth. The central wavelength of the source could be continuously and accurately temperature-tuned to wavelengths in and around the

FBG band gap.

Initially the nonlinear self-switching of a single input beam was studied. All of the power from the source was directed into beam A and WP2 used to control the power incident on the grating. With the beam launched on a single birefringence axis (axis 1) of the FBG, the signal wavelength was temperature tuned into the strongly reflective (>95% reflectivity), short wavelength region of the bandgap (see figure 2). At low powers the FBG was highly reflective however as the peak power was increased a sharp nonlinear increase in energy transmission through the grating was observed. The increased transmission was a result of the generation of a single gap soliton. The soliton formed typically 1ns after the chirped spike marking the leading edge of the incident pulse and had a duration of ~ 500ps. The exact threshold for this nonlinear switching was dependant on the precise position within the bandgap and increased as the laser was tuned further into the bandgap as expected. The minimum value of threshold was found to be around 1.25 kW. When the incident beam was then launched onto the orthogonal FBG birefringence axis (axis 2) similar gap soliton formation was observed. However, the shift in the central Bragg wavelength due to the fibre birefringence (see figure 2) meant that the exact threshold for nonlinear transmission at any one wavelength was observed to be different on the two axes.

We next examined operation of the system as an 'AND' gate. The laser frequency was temperature tuned to the position indicated in Fig.2 and equal powers launched in each input beam. In fig.3 we plot the transmitted pulse profiles for the FBG for an estimated launched power of 2.5 kW per beam. Traces A and B show the profiles for each input beam, A (on axis 1) and B (on axis 2), individually incident in isolation. The first two short temporal features seen in Figure 3 were found to be due to the sharp leading edge spike of the incident pulse and could be ignored, leaving only a low level signal accounting for a few percent of the input pulse energy. These cases correspond to '0+1' and '1+0' inputs to the 'AND' gate. Figure 3C was obtained with both beams simultaneously launched into the FBG, corresponding to a '1+1' gate input. In this instance a significant, nonlinearly switched coupled gap soliton pulse of 500ps duration is seen to form approximately 1ns after the spike marking the front edge of the incident pulses. Calculating the energy contained in the pulses for traces a-c (excluding that contained in the leading spikes) shows a switching contrast of ≈10dB for the 'AND' gate. The contrast was found to be highly dependent on the wavelength of the incident beams relative to the bandgap of the FBG and operated at this contrast level only over a narrow frequency range (~100MHz). As the signal was moved further into the bandgap gap soliton formation ceased while moving towards the edge of the bandgap gap soliton by the individual channels was observed.

Improvements in the switching contrast were obtained by adding a polariser at the output of the FBG. This allowed us to obtain preferential selection of a single polarisation component of the switched pulse. Switching contrasts as high as 17dB were obtained (once again evaluated by excluding the contribution leading edge spike).

The switching behaviour was further studied by varying the power incident in beam A whilst keeping that in beam B constant, the transmitted pulse energy was recorded and is presented in figure 4. At low (but still nonlinear) powers the output was seen to intially follow a roughly exponential increase with the peak power launched in arm A, however, between 2.4kW and 2.6kW a distinct jump in the transmission was observed. The jump was clearly observed to be associated with the formation of gap solitons within the bandgap of the FBG, resulting in the transmitted pulse observed in figure 3C.

In conclusion, we have demonstrated the operation of an all-optical 'AND' gate based on the formation and transmission of coupled gap solitons through a FBG. A switching contrast of close to 17dB between zero and one output states was observed. The operation of the gate required input pulse peak powers above 2kW. The transmitted 500ps switched pulse and the accompanying sharp jump in transmitted energy confirm that the formation of gap solitons within the bandgap of the FBG was the switching mechanism in this system. Although the results presented here represented switching of nanosecond pulses, similar results should be achievable with far shorter pulses. The main requirement for the operation of this system (apart from sufficient peak power) is a FBG of greater bandwidth and similar length to that of the pulse. Hence, as the pulse width is reduced shorter gratings of increased modulation depth would be required.

References

[1] C. Martijn de Sterke. J. E. Sipe: Progress in OpticsXXXIII, 1994, E. Wolf, ed., pp203-260, (Elsevier, Amsterdam, 1994).

[2] W. Chen, D. L. Mills: Phys. Rev. Lett., 1987, 58, 2, 160-163.

[3] N. G. R. Broderick, C. M. de Sterke, J. E. Sipe: Op. Comm., 1994, 113, 118-124.

[4] D. Taverner, N. G. R. Broderick, D. J. Richardson, R. I. Laming, M. Ibsen: Conf. Bragg Gratings, Photosensitivity, and Poling in Glass Fibers and Waveguides, Williamsburg, Oct, 1997, paper BMB3.

[5] S. Lee, S. T. Ho: Opt. Lett., 1993, 18, 12, 962-964.

[6] W. Samir, S. J. Garth, C. Pask: J. Opt. Soc. Am. B, 1994, 11, 1, 64-71.

[7] M. J. Cole, W. H. Loh, R. I. Laming, M. N. Zervas, S. Barcelos: Electron. Lett., 1995, 31, 17, 1488-1490.

[8] D. Taverner, D. J. Richardson, L. Dong, J. E. Caplen, K. Williams, R. V. Penty: Opt. Lett., 1997, 22, 6, 378-380.

Captions

Figure 1: Experimental setup. LA-EDFA: Large mode-area erbium-doped fibre amplifier. WP1, WP2, WP3: Waveplates. FBG: Fibre Bragg grating. PBS: Polarisation beam-splitter. POL: Optional polarizer. The directly detected (≈50ps resolution) input pulse temporal profile is shown inset.

Figure 2: Reflection time-delay and amplitude response measurements made on the two birefringence axes of the FBG. The vertical dashed line represents the incident signal wavelength. for the traces shown in figure 3.

Figure 3: Directly detected (≈50ps resolution) transmitted pulse intensity profiles for each individual input beam (A, B) and both beams simultaneously (C).

Figure 4: Transmitted pulse energy varying with launched peak power in beam A. The peak power in beam B was held constant at 2.8kW. The solid line represents an exponential fit to the sub-1.5kw data points, demonstrating the jump in transmission observed at the point of gap soliton formation (2.4-2.6kw).

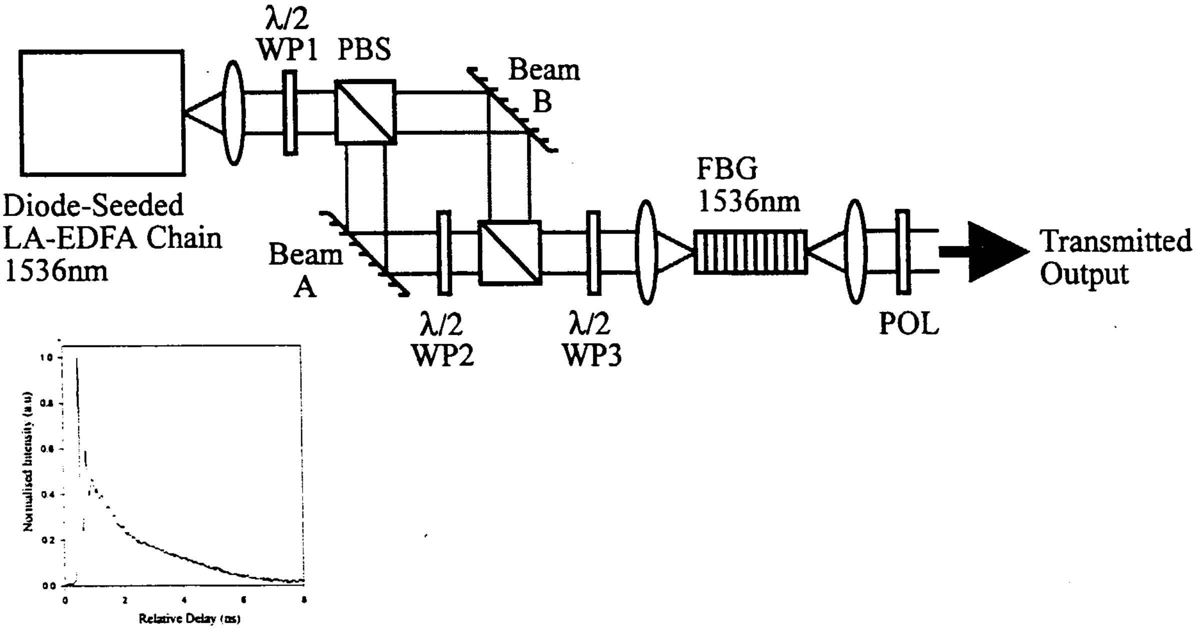
λ/2
WP1
PBS
Beam
B
Diode-Seeded
LA-EDFA Chain
1536nm
Beam
A
λ/2
WP2
λ/2
WP3
FBG
1536nm
POL
Transmitted
Output
Normalised Intensity (a.u)
Relative Delay (ns)

Figure 1

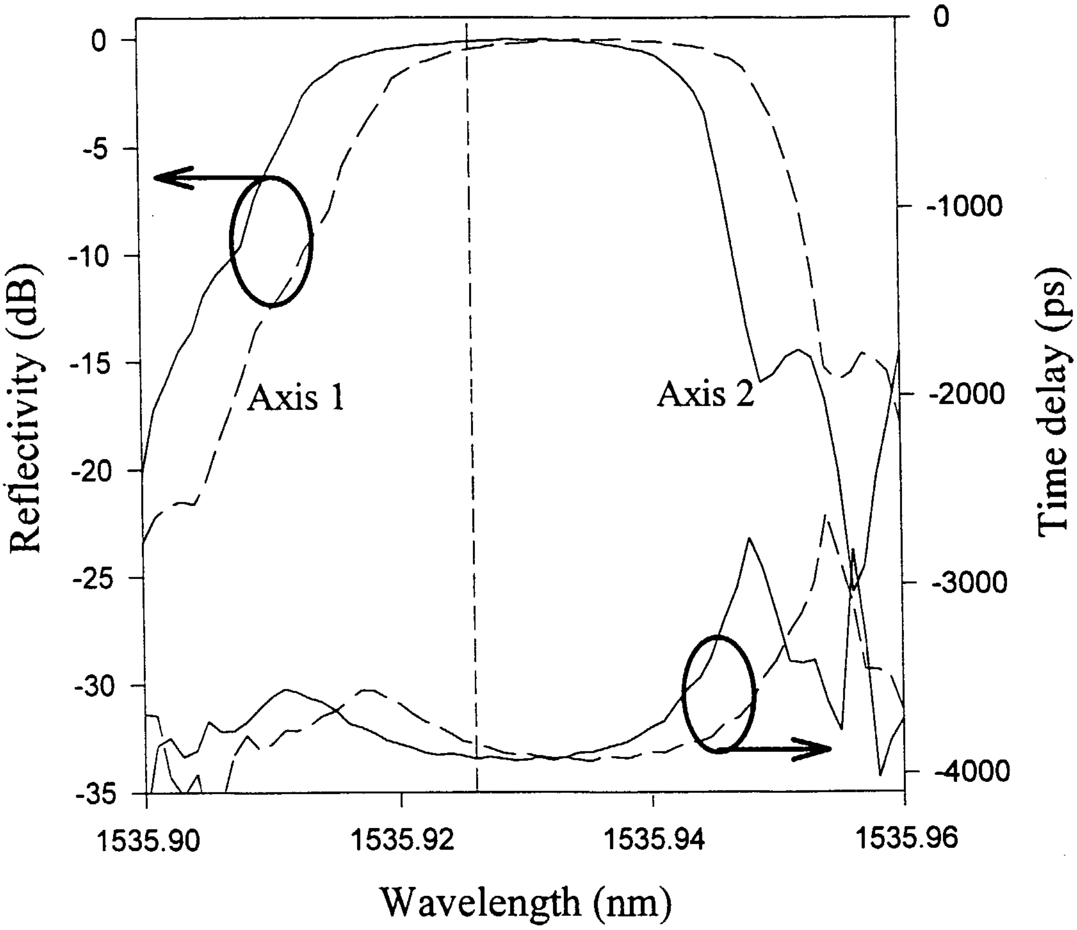

0
-5
-10
-15
-20
-25
-30
-35
Reflectivity (dB)
Axis 1
Axis 2
0
-1000
-2000
-3000
-4000
Time delay (ps)
1535.90
1535.92
1535.94
1535.96
Wavelength (nm)

figure 2

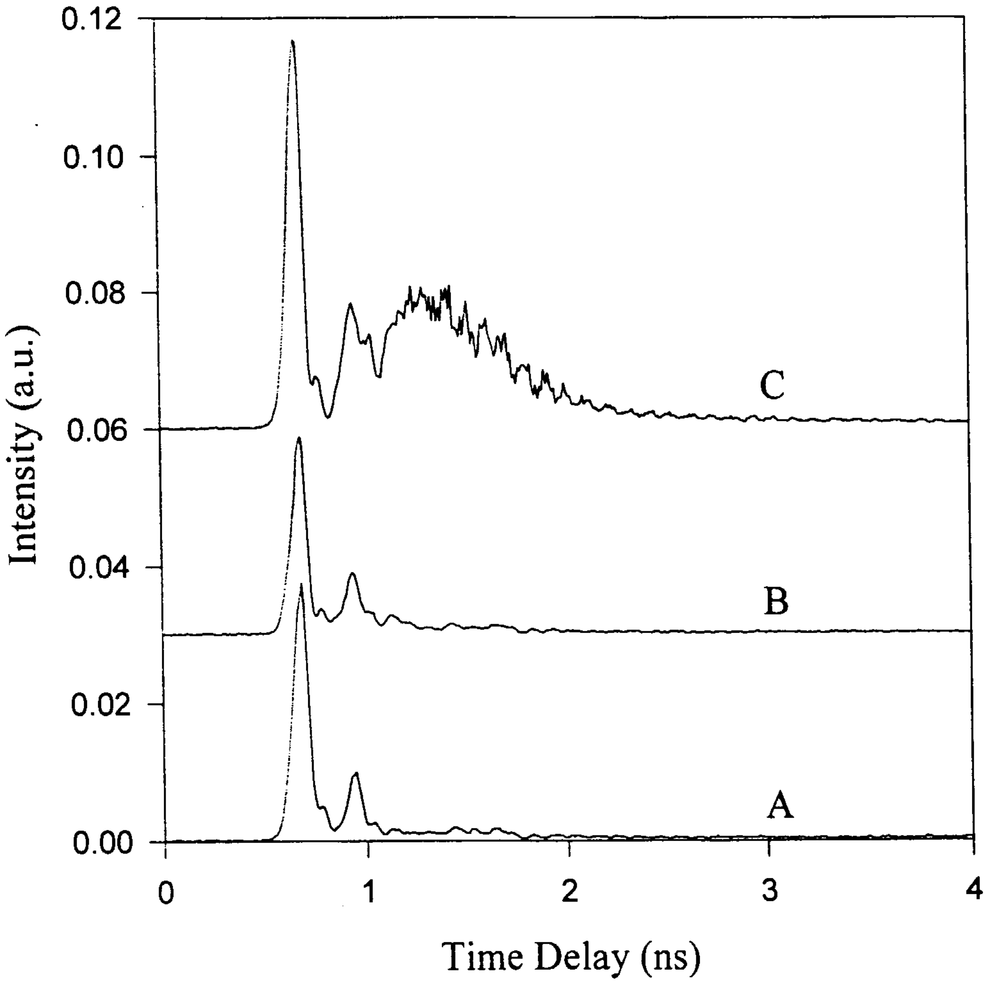
0.12
0.10
0.08
0.06
0.04
0.02
0.00
Intensity (a.u.)
C
B
A
0
1
2
3
4
Time Delay (ns)

figure 3

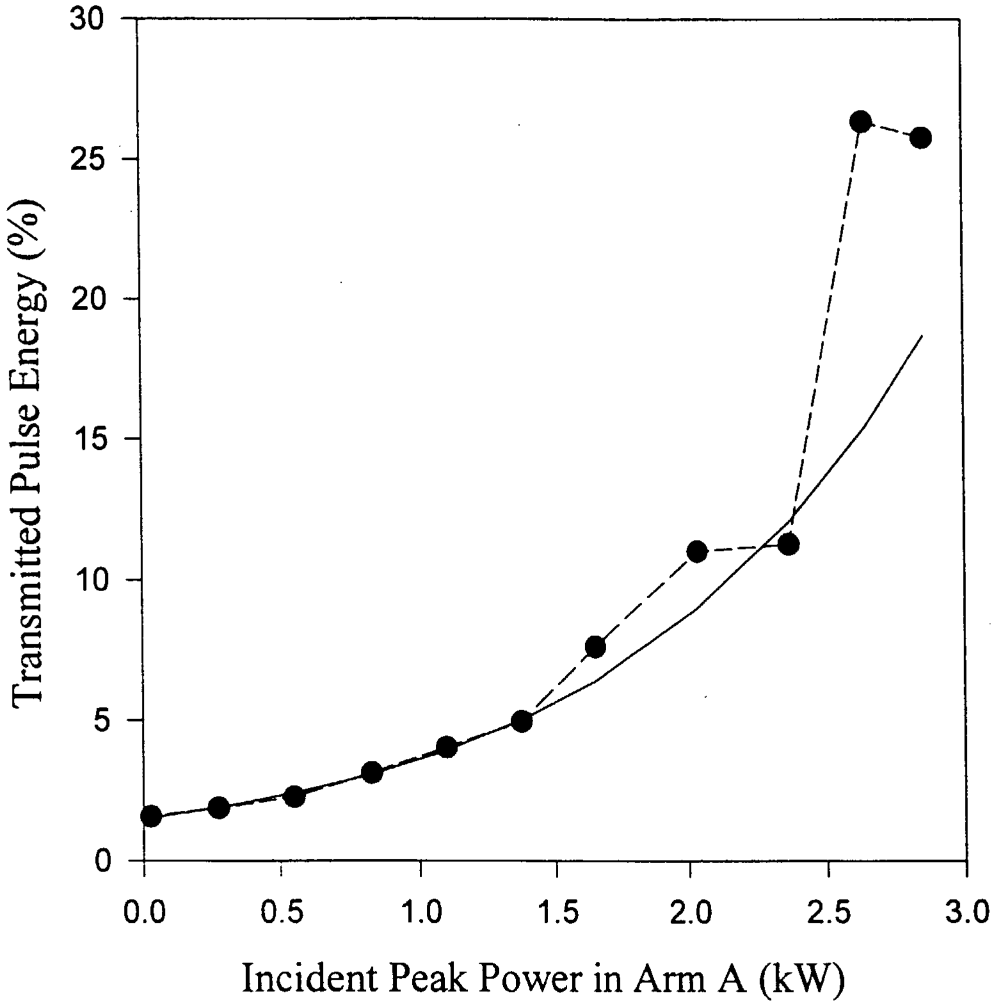
30
25
20
15
10
5
0
0.0
0.5
1.0
1.5
2.0
2.5
3.0
Transmitted Pulse Energy (%)
Incident Peak Power in Arm A (kW)

figure 4